Selfconsistent evaluation of charm and charmonium in the quark-gluon plasma

New Journal of Physics
The open-access journal for physics

Selfconsistent evaluation of charm and charmonium in the quark-gluon plasma

F Riek and R Rapp
Cyclotron Institute, Texas A&M University, College Station, TX 77843-3366, USA
E-mail: friek@comp.tamu.edu and rapp@comp.tamu.edu

New Journal of Physics **13** (2011) 045007 (20pp)
Received 30 November 2010
Published 8 April 2011
Online at http://www.njp.org/
doi:10.1088/1367-2630/13/4/045007

Abstract. A selfconsistent calculation of heavy-quark (HQ) and quarkonium properties in the quark-gluon plasma (QGP) is conducted to quantify flavor transport and color screening in the medium. The main tool is a thermodynamic T-matrix approach to compute HQ and quarkonium spectral functions in both scattering and bound-state regimes. The T-matrix, in turn, is employed to calculate HQ selfenergies which are implemented into spectral functions beyond the quasiparticle approximation. Charmonium spectral functions are used to evaluate Eulcidean-time correlation functions, which are compared to results from thermal lattice QCD. The comparisons are performed in various hadronic channels, including zero-mode contributions consistently accounting for finite charm-quark width effects. The zero modes are closely related to the charm-quark number susceptibility, which is also compared to existing lattice 'data'. Both the susceptibility and the heavy-light quark T-matrix are applied to calculate the thermal charm-quark relaxation rate, or, equivalently, the charm diffusion constant in the QGP. Implications of our findings in the HQ sector for the viscosity-to-entropy-density ratio of the QGP are briefly discussed.

Contents

1. Introduction

In recent years rather remarkable properties of the quark-gluon plasma (QGP) have been discovered, notably a liquid-like behavior deduced from the collective expansion of the medium formed in collisions of heavy nuclei at the Relativistic Heavy Ion Collider (RHIC). Hydrodynamic expansion models, based on the assumption of local thermal equilibrium, require very short equilibration times, of the order of $\tau_{\rm therm} \simeq 1\,{\rm fm}/c$ or less, to account for the experimental findings. The microscopic origin of the rapid thermalization remains one of the outstanding problems raised by the RHIC data. It is further complicated by the fact that the very notion of equilibrium erases information about its origin. A phenomenologically suitable probe of thermalization in heavy-ion collisions should therefore interact strongly at the thermal scale, but with a relaxation time on the order of the system's lifetime (at RHIC, $\tau_{\rm QGP} \simeq 5\,{\rm fm}/c$). The logical choice is thus heavy quarks, i.e. charm and bottom ($Q = c, b$), for which thermalization is expected to be delayed by a factor m_Q/T, quite comparable to $\tau_{\rm QGP}/\tau_{\rm therm}$ (see e.g. [1] for a recent review).

Bound states of heavy quarks (charmonia and bottomonia) are believed to probe the QGP from a somewhat different angle [2]–[6]. The dissolution pattern of the quarkonium spectrum in matter is possibly the most direct way of diagnosing color-Debye screening of the basic QCD force, $\mathbf{f}_{Q\bar{Q}} = -\nabla V_{\bar{Q}Q}(r)$, as a function of temperature (and/or density). In-medium quarkonium spectroscopy therefore reveals insights into the deconfining hadron-to-parton phase transition in QCD. In particular, the use of potential models has been revived recently, largely triggered by the prospect that an in-medium potential can be extracted model-independently from lattice QCD (lQCD) computations. Furthermore, lQCD generates Euclidean-time (τ) correlation functions of quarkonia with good accuracy in different hadronic channels, which provide useful constraints on model calculations of spectral functions in the timelike regime of physical excitations. The extraction of reliable information from such comparisons requires a realistic modeling of the continuum part (scattering regime) of the quarkonium spectral

functions, i.e. not only its bound-state part. The account of interactions in the near-threshold region is particularly important to describe situations where bound states dissolve into the continuum, as in the case at hand. In connection with correlator analyses, a comprehensive treatment of bound-state and continuum regimes has been performed using Schrödinger phase shifts [7], a thermodynamic T-matrix [8] or a nonrelativistic Green's function [9] approach. Another important ingredient for a realistic description of quarkonium spectral functions in the QGP is medium effects in the single-particle properties, i.e. in the heavy-quark (HQ) propagation. These are closely related to HQ transport [10, 11] and the so-called zero-mode contributions to quarkonium spectral and correlation functions [12, 13]. In particular, finite-width effects on both quarkonia and heavy quarks have received little attention thus far [8, 14].

In the present paper we further develop our previous study of heavy quarks and quarkonia in the QGP using a thermodynamic T-matrix approach [10]. First, we go beyond the quasiparticle approximation for heavy quarks and perform a selfconsistent calculation of the HQ selfenergy and the in-medium heavy-light T-matrix. The improved HQ spectral functions are then implemented into an off-shell calculation of the quarkonium spectral functions. Secondly, we expand our comparison with Euclidean correlator ratios to the scalar, vector and axialvector channels. In these channels the presence of zero modes [12, 13], resulting from scattering of a single heavy quark on medium constituents ('particle–hole' excitations), is known to impact the large-τ behavior of the in-medium correlators appreciably. Thus far, these contributions have been estimated in quasiparticle approximation neglecting finite width effects [9, 12, 13, 15, 16]. In a treatment of heavy quarks consistent with the T-matrix we evaluate the zero-mode contribution accounting for their full spectral function, in particular finite-width effects. This automatically yields predictions for the charm-quark number susceptibility, which can be compared to lattice data and enable a more reliable extraction of in-medium quasiparticle masses for heavy quarks.

The paper is organized as follows. In section 2 we give a short overview of the T-matrix formalism employed in our calculations, specifically discussing its extension to off-shell dynamics in the charm-quark propagation. Section 3 is devoted to properties of charmonia in the QGP, i.e. their spectral functions including zero modes (section 3.1), Euclidean correlator ratios in various mesonic channels (section 3.2) and a comparison of numerical results to lQCD data using two different input potentials (section 3.3). In section 4 we first analyze the selfconsistently calculated charm-quark selfenergies (section 4.1) and then apply these to obtain the thermal relaxation rate and a schematic estimate of η/s (section 4.2), as well as the charm-quark number susceptibility (section 4.3). We conclude in section 5.

2. Off-shell T-matrix at finite temperature

The formalism for calculating the T-matrix for quark-quark and quark-antiquark scattering and bound states in the QGP, using two-body potentials estimated from HQ free energies computed in lQCD, has been developed in [8, 10, 17]. Here we recollect the main elements while referring to [10] for further details (e.g. a discussion of relativistic corrections and constraints from vacuum spectroscopy and the high-energy perturbative limit). The starting point is the Bethe–Salpeter equation, which after a three-dimensional (3D) reduction and partial-wave expansion turns into a 1D integral equation for the scattering amplitude (T-matrix),

$$T_{l,a}(E;q',q) = \mathcal{V}_{l,a}(q',q) + \frac{2}{\pi}\int_0^\infty \mathrm{d}k\, k^2\, \mathcal{V}_{l,a}(q',k) G_{12}(E;k)\, T_{l,a}(E;k,q), \tag{1}$$

in a given color channel (a) and partial wave (l); the relative three-momentum moduli of the initial, final and intermediate two-particle state are denoted by $q = |\mathbf{q}|$, $q' = |\mathbf{q}'|$ and $k = |\mathbf{k}|$, respectively (we restrict ourselves to vanishing total three-momentum, $\mathbf{P} = 0$, of the two-particle system). The explicit form of the intermediate two-particle propagator, G_{12}, depends on the 3D reduction scheme [18]–[21] (in slight deviation from [8, 10, 17] we here absorb the Pauli blocking factor, $(1 - 2f_F)$, into G_{12}). In the following, we focus on the Thompson scheme, since the Blankenbecler–Sugar scheme was found to generate some overbinding in the vacuum quarkonium spectrum [10]. The T-matrix will be applied in both heavy-heavy and heavy-light quark channels for which a static (potential) approximation can be justified (i.e. the energy transfer is parametrically suppressed compared to the three-momentum transfer, $\Delta q_0 \sim (\Delta\mathbf{q})^2/m_Q \ll \Delta q$, where $\Delta\mathbf{q} = \mathbf{q}' - \mathbf{q}$). For the two-body potential, $\mathcal{V}_{l,a}$, we follow our previous work [10] using either the heavy-quark free (F) or internal (U) energy computed in lQCD, implemented into a field-theoretical model for color-Coulomb and confining terms [22] with relativistic corrections (e.g. the Breit interaction [23]–[25] to account for color-magnetic effects). To ensure the convergence of the Fourier transform from coordinate to momentum space we subtract the infinite-distance limit of the potential according to

$$V_a(r;T) = X_a(r,T) - X(r\to\infty,T), \qquad X = F \text{ or } U, \tag{2}$$

and interpret $X_\infty(T)/2 \equiv X(r\to\infty,T)/2$ as a temperature-dependent correction to the bare HQ mass (real part of selfenergy) induced by the condensate associated with the confining force term. The use of either U or F as potential is believed to bracket the uncertainties in this identification.

2.1. Two-particle propagator

In all previous applications of potential models in the QGP the quarks have been treated as quasiparticles with either vanishing or constant [8, 10] width. However, as pointed out in [10], this approximation implies that quarkonium spectral functions, $\rho_\alpha(E)$ (α: quantum numbers of the composite mesonic (or diquark) state), do not possess the proper low-energy limit, $\rho_\alpha(E\to 0) \propto E$. While this is not expected to significantly impact the mass and binding energy of the bound states (for which the total energy is of order twice the HQ mass), the Euclidean correlators calculated below involve an integration over $\rho_\alpha(E)$ starting from $E = 0$ with a thermal weight which diverges for $E \to 0$. In previous studies this problem has been evaded by introducing a low-energy cutoff on the spectral function (sufficiently below the lowest bound state as to not affect the correlator). However, recent studies of quark spectral functions [26] find considerable low-energy strength in quarkonium spectral functions, e.g. due to particle–hole like structures in the HQ propagator. Thus a more elaborate treatment in the T-Matrix equation, properly accounting for off-shell dynamics, is in order.

The general off-shell expression of the uncorrelated 2-fermion propagator at finite temperature, G_{12}, figuring into the T-matrix equation, can be derived, e.g. within the Matsubara formalism. One has

$$G_{12}(\Omega_\lambda, k) = T\sum_\nu G_1(z_\nu, \mathbf{k}) G_2(\Omega_\lambda - z_\nu, -\mathbf{k}), \tag{3}$$

where

$$G_i(\omega, \mathbf{k}) = \frac{1}{\omega^2 - k^2 - m_i^2 - 2m_i\Sigma_i(\omega,k)} \tag{4}$$

($i = 1, 2$) denotes the scalar part of the one-particle propagator, and $z_\nu = i(2\nu+1)\pi T$ (Ω_λ) are fermionic (bosonic) Matsubara frequencies. Using the spectral representations of the in-medium (retarded) single-particle propagators,

$$G_i(\omega, \mathbf{k}) = \int \frac{\mathrm{d}\omega'}{2\pi} \frac{\rho_i(\omega', k)}{\omega - \omega'}, \quad \rho_i \equiv -2\,\mathrm{Im}\, G_i, \tag{5}$$

the Matsubara summation in equation (3) can be performed explicitly. After analytic continuation to the real axis ($\Omega_\lambda \to E$), the positive-energy contributions to the two-particle propagator take the form

$$G_{12}(E, k) = \int \frac{\mathrm{d}\omega}{\pi} \int \frac{\mathrm{d}\omega'}{\pi} \rho_1^+(\omega, k)\, \rho_2^+(\omega', k)\, m_1\, m_2\, \frac{1 - f_F(\omega) - f_F(\omega')}{E - \omega - \omega' + \mathrm{i}\,\epsilon}, \tag{6}$$

where

$$\rho_i^+(\omega, k) = \frac{-1}{\omega_i(k)} \mathrm{Im} \frac{1}{\omega - \omega_i(k) - \Sigma_i(\omega, k)}, \ \omega_i(k) = \sqrt{k^2 + m_i^2} \tag{7}$$

denotes the positive-energy part of the quark spectral functions. The factor $m_1 m_2$ in equation (6) is specific to the Thompson reduction scheme, rendering the appropriate expression for G_{12} in the limit of on-shell quarks [21]. For the in-medium HQ mass, as mentioned above (recall equation (2)), the infinite-distance value of the HQ potential is identified with a 'mean-field' contribution, i.e. as a real part of a selfenergy,

$$m_Q = m_Q^0 + \Sigma_Q^{\mathrm{MF}}(T), \quad \Sigma_Q^{\mathrm{MF}}(T) \equiv X_\infty(T)/2. \tag{8}$$

We neglect (momentum-dependent) HQ selfenergy contributions from scattering off thermal gluons. The additional selfenergy figuring into the quark propagator in equation (7) is generated from interactions with thermal light quarks and antiquarks and is therefore distinct from $X_\infty(T)$. It will be computed from the heavy-light quark T-matrix, as discussed below. For calculating the latter, we need to specify the light-quark masses, which we model by a thermal mass proportional to gT with a coefficient to approximately match lQCD computations of the energy density of the QGP in quasiparticle approximation. In addition, we supplement a moderate imaginary part for the light-quark selfenergy, $\mathrm{Im}\,\Sigma_q = -0.05\,\mathrm{GeV}$, which is in the range of values obtained in [17] in a similar approach for light quarks, and comparable to what we obtain for heavy quarks. It is also comparable to results of the dynamical quasiparticle approach [27] close to T_c, where $\Gamma_q \simeq 0.1\,\mathrm{GeV}$ (increasing to about $0.2\,\mathrm{GeV}$ at $2\,T_c$), albeit in this approach the effect from thermal gluons is larger (our results for quarkonium spectral function and HQ transport are, however, largely insensitive to the light-quark width [14]).

The evaluation of the Matsubara sum in equation (3) also generates a contribution that solely arises from thermal excitations (see, e.g. [28]). It involves one positive- and one negative-energy part of the quark spectral functions which is why we referred to it as a 'particle-hole' contribution above. For mesonic channels of the T-matrix, $12 = Q\bar{Q}$, its imaginary part can be cast into the form

$$\mathrm{Im}\, G_{12}^{\mathrm{ph}}(E, k) = -\int \frac{\mathrm{d}\omega}{2\pi} \rho_Q^+(\omega, k) \rho_{\bar{Q}}^+(E + \omega, k) [f^Q(\omega, k) - f^{\bar{Q}}(E + \omega, k)]. \tag{9}$$

Here, the negative-energy part of the $\bar{Q}$ spectral function has been turned into the positive-energy part of the Q spectral function, i.e. the $\bar{Q}$ line in the original $Q\bar{Q}$ propagator has been 'turned around'. Together with the Fermi distributions, the interpretation of this contribution to G_{12} becomes apparent: an incoming Q, pre-existing in the heat bath according to $f^Q(\omega, k)$,

scatters into a Q with energy $E+\omega$, Pauli-blocked according to $f^Q(E+\omega,k)$. $G_{12}^{\rm ph}$ is, in fact, precisely the zero-mode contribution discussed in the context of quarkonium correlators [9, 12, 13, 15]. We return to its evaluation in section 3.1 below.

2.2. Single-quark selfenergy

The HQ selfenergy, $\Sigma_Q(\omega,k)$, due to interactions with light anti-/quarks in the heat bath, is calculated from the heavy-light (Qq) T-Matrix by closing its light-quark line with a quark propagator weighted with a Fermi distribution function. Using the Matsubara formalism one can express its imaginary part as [17, 28]

$$\begin{aligned}\mathrm{Im}\,\Sigma_Q(\omega,k) = \frac{\mathrm{d}_{SI}}{6k}\int\frac{p\,\mathrm{d}p}{(2\pi)^2}\int_{E_{\rm min}}^{E_{\rm max}} E\,\mathrm{d}E\,\mathrm{Im}\,M_{qQ}(E,\omega,\omega_q(p),k,p)\\ \times[f_F(\omega_q(p))+f_{\rm B}(\omega+\omega_q(p))]\end{aligned} \tag{10}$$

with

$$M_{qQ}(E,\omega,\omega',k,p) = \frac{m_q\,m_Q}{\omega_q(q_{cm})\,\omega_Q(q_{cm})}\,4\pi\sum_{a=1,8} d_a[T_{a,0}(E,q_{cm})+3T_{a,1}(E,q_{cm})], \tag{11}$$

where

$$\begin{aligned} q_{cm}^2(E,k_{(4)},p_{(4)}) &= \frac{(E^2-k_{(4)}^2-p_{(4)}^2)^2-4k_{(4)}^2\,p_{(4)}^2}{4E^2},\\ k_{(4)}^2 &= \omega^2-k^2,\quad p_{(4)}^2=\omega'^2-p^2,\\ E_{\rm min}^2 &= (\omega+\omega')^2-(k+p)^2,\\ E_{\rm max}^2 &= (\omega+\omega')^2-(k-p)^2. \end{aligned} \tag{12}$$

The spin–isospin factor $d_{\rm SI}=4N_f$ counts the degeneracy of available meson (or diquark) states, e.g. with total spin-0 and -1 for S-wave heavy-light scattering [14]. In the expression for the HQ selfenergy, equation (10), the thermal light quarks are treated as zero-width quasiparticles so that their spectral functions can be replaced by δ functions (but with thermal mass $\sim gT$)[1]. We recall that the gluonic contributions are entirely attributed to the mean-field type condensate term (for HQ transport, we include HQ–gluon interactions to leading order in perturbation theory which does not generate an imaginary part in the scattering amplitude). The real part of the selfenergy is obtained by a dispersion relation which is a preferred procedure in a selfconsistent treatment since the normalization of the spectral functions can easily be guaranteed. Our framework is similar to the one utilized in [17] in the light-quark sector. However, in there the calculations of the T-matrix were restricted to on-shell selfenergies, while here we use the full off-shell selfenergy of the heavy quark which, in particular, enables to establish the correct low-energy behavior of the mesonic spectral functions (in addition to refinements in the implementation of the potential, as developed in [10], the nonpotential corrections are expected to be significantly larger for light-quark interactions).

Let us finally comment on relations of imaginary parts in the two-body potential and the single-quark selfenergy. Using effective field theory (EFT) at finite temperature it has been found that the two-body potential operator figuring into a Schrödinger equation acquires an

[1] This is mainly done for numerical reasons. We have checked that using an off-shell quark spectral function leads to very similar results.

imaginary part [29]–[32]. Diagrammatically, this implies that the potential possesses on-shell cuts corresponding to dissociation processes of the composite (bound) state. In combination with weak coupling techniques, two types of thermal dissociation contributions have been identified for small binding energies, $E_B \ll T$, $m_D \sim gT$, one originating from Landau damping in the (spacelike) one-gluon exchange and the other one due to so-called color-singlet-to-octet transitions [30]. The former dominates over the latter if $E_B \ll m_D$ (as relevant for excited states or the case of reduced in-medium J/ψ binding energies close to its dissolution temperature). Landau damping is also the origin of the imaginary part of the two-body potential discussed in [29, 31, 32]. The actual process is a scattering (or 'quasifree') dissociation [34], $p + J/\psi \to p + c + \bar{c}$, induced by thermal partons $p = g, q, \bar{q}$ (which generate the imaginary part of the one-loop selfenergy of the exchanged gluon). In the limit of small binding (or large charmonium size), the incoming thermal partons with energy $\sim T$ do not sense the size of the bound state and thus the scattering effectively happens on an individual charm (or anti-charm) quark. In the T-matrix formalism this process is encoded in the selfenergy of a single (anti-) charm quark, which is included in our calculations. For larger binding energies the singlet-to-octet mechanism, induced by absorption of a thermal gluon, becomes competitive and eventually dominant; for $E_B \geqslant T$ the EFT potential becomes real and imaginary parts figure through loop corrections, with the leading contribution from the singlet-to-octet break-up [30]. Diagrammatically, it corresponds to the gluo-dissociation process, $g + J/\psi \to c + \bar{c}$, first analyzed by Bhanot and Peskin [33] (up to final-state interactions in the octet channel, which, however, are suppressed by $1/N_c^2$ and thus numerically negligible). In our T-matrix formalism, the inclusion of this process would require a coupled-channel treatment, with a $c\bar{c}$-gluon intermediate state, whose cut produces the corresponding decay channel. Such a calculation is beyond the scope of the present work. Naively, gluo-dissociation is of lower order in α_s than quasifree dissociation, but the former runs out of phase space for small E_B [34]. For large binding, quasifree dissociation ceases since the thermal parton does not resolve the substructure of the color neutral bound state [29, 31]. When formulated as a potential contribution, the large-distance limit of its imaginary part coincides with twice the imaginary part of the charm-quark selfenergy [29]. Therefore our T-matrix calculations using a real potential are well in line with the use of a complex potential in a Schrödinger treatment. In the T-matrix, imaginary parts are generated via unitarization of intermediate (on-shell) states including single-particle selfenergy contributions.

3. Quarkonia

In this section we apply the selfconsistent T-matrix to charmonia with special consideration of the zero-mode contribution (section 3.1) to the Euclidean correlators in different mesonic channels, $\alpha = S, PS, V, AV$, i.e. scalar, pseudoscalar, vector and axialvector, respectively (section 3.2), followed by a discussion of numerical results using either U or F as underlying two-body potential (section 3.3).

3.1. Spectral functions and zero modes

With the $c\bar{c}$ T-matrix from equation (1) we proceed to determine the charmonium spectral function including both bound and scattering states, as in [10]. The T-matrix signifies the

rescattering contribution to the correlation function, which is schematically given by [8]

$$G = G^0 + G^0\, T\, G^0, \tag{13}$$

where G^0 denotes the free two-particle loop. This can be be represented diagrammatically as

$G =$ 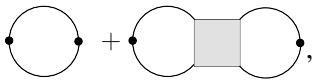 , (14)

where compared to equation (6) the loop now also includes an integration over relative momentum, $\mathbf{k}$, as well as vertices (denoted by dots) specifying the quantum-number channel α. The spectral function is then defined as usual by $\rho = -2\,\mathrm{Im}\, G$.

Quantitative comparisons to Euclidean correlator ratios as 'measured' in lQCD [35, 36] require the inclusion of zero-mode contributions [12, 13], which turn out to be different for different meson channels α. This, in particular, lifts the spin degeneracy within S-wave ($PS-V$) and P-wave ($S-AV$) states of the T-matrix. This is not surprising since HQ symmetry is not expected to be valid for zero modes. A relativistic evaluation of the vertices figuring into $\rho_\alpha^{\mathrm{zm}} \equiv -2\,\mathrm{Im}\, G_\alpha^{\mathrm{ph}}$ is therefore in order. To be consistent with the treatment of the T-Matrix we evaluate this contribution beyond the zero-width quasiparticle approximation (as applied in the literature to date) by taking into account the finite width of the quark. As in previous literature, we focus on the leading part of the zero-mode contribution, which does not involve a two-body potential contribution[2]. Augmenting equation (9) with relativistic vertices one obtains [12]

$$\begin{aligned}\rho_\alpha^{\mathrm{zm}}(P) &= 2N_c \int \frac{\mathrm{d}^4k}{(2\pi)^4}\, \mathrm{Tr}[(\not{k}+m_c)\,\Gamma\,(\not{r}+m_c)\,\Gamma^\dagger] \times\ \rho_c^+(k)\,\rho_c^+(r)\,[f^F(k^0)-f^F(r^0)] \\ &= 2N_c \int \frac{\mathrm{d}^4k}{(2\pi)^4}\, 4\,F_\Gamma(k,r,m_c) \times\ \rho_c^+(k)\,\rho_c^+(r)\,[f^F(k^0)-f^F(r^0)],\end{aligned} \tag{15}$$

where we introduced the notation

$$r = P + k, \quad \Gamma \in \{1, \gamma_5\,, \gamma_0, \gamma_i, \gamma_5\gamma_i\}, \tag{16}$$

with r, k and $P = (E, \mathbf{P})$ denoting 4-vectors for the purposes of the above two and the following equation only. The kinematic factors arising from the different Dirac structures take the form

$$\begin{aligned} F_1(k,r,m) &= k\cdot r + m_c^2, \\ F_{\gamma_5}(k,r,m) &= k\cdot r - m_c^2, \\ F_{\gamma_0}(k,r,m) &= k_0\cdot r_0 + \mathbf{k}\cdot\mathbf{r} + m_c^2, \\ F_{\gamma_i}(k,r,m) &= 3\,r^0k^0 - \mathbf{r}\cdot\mathbf{k} - 3m_c^2, \\ F_{\gamma_5\gamma_i}(k,r,m) &= 3\,r^0k^0 - \mathbf{r}\cdot\mathbf{k} + 3m_c^2; \end{aligned} \tag{17}$$

a summation over spatial indices i is implied for the vector and axialvector case. In the previously adopted zero-width approximation the zero-mode spectral function can be simplified to [12]

$$\rho_\alpha^{\mathrm{zm}}(E, \mathbf{P}\to 0) = 2\pi\, E\, \delta(E)\chi_\alpha(T), \tag{18}$$

[2] A nonperturbative treatment of the particle–hole interaction would require a relativistic treatment solving the Bethe–Salpeter equation, which goes beyond the potential approximation adopted here.

where

$$\chi_\alpha(T) = -2N_c \int \frac{\mathrm{d}^3\mathbf{k}}{(2\pi)^3}\left(c_1 + c_2\frac{\mathbf{k}^2}{\omega_c(\mathbf{k})^2}\right)\frac{\partial f^c(\omega_c(\mathbf{k}))}{\partial\omega_c(\mathbf{k})} \tag{19}$$

denotes a generalized susceptibility with coefficients corresponding to different quantum number channels according to

$$\begin{aligned}
&\Gamma = 1 \Rightarrow c_{1,2} = 2, -2, \qquad &&\Gamma = \gamma_5 \Rightarrow c_{1,2} = 0, 0,\\
&\Gamma = \gamma_0 \Rightarrow c_{1,2} = 2, 0, \qquad &&\Gamma = \gamma_i \Rightarrow c_{1,2} = 0, 2,\\
&\Gamma = \gamma_5\gamma_i \Rightarrow c_{1,2} = 6, -4.
\end{aligned}$$

In our numerical calculations reported below we evaluate $\rho_\alpha^{\mathrm{zm}}$ directly from equation (15) using the positive-energy charm-quark spectral function, equation (7), with the selfconsistently determined off-shell selfenergy. This puts the treatment of the zero-mode contribution on the same level as the $c\bar{c}$ scattering and bound-state part using the two-particle propagator G_{12} in equation (6).

3.2. Euclidean correlator ratios

The transformation of the spectral function to the Euclidean correlator is given by

$$\begin{aligned}
G_\alpha(\tau, T) &= \int \frac{\mathrm{d}E}{2\pi}\left[\rho_\alpha(E, T) + \rho_\alpha^{\mathrm{zm}}(E, T)\right]\mathcal{K}(\tau, E, T),\\
\mathcal{K}(\tau, E, T) &= \frac{\cosh[E\,(\tau - 1/2T)]}{\sinh[E/2T]}.
\end{aligned} \tag{20}$$

As before, we focus an vanishing total three-momentum, $\mathbf{P} = 0$, of the $Q\bar{Q}$. The temperature kernel $\mathcal{K}$ imprints an exponential τ dependence on the correlator. To better exhibit the in-medium modifications of $G_\alpha(\tau, T)$ it is therefore common to analyze the correlator ratio

$$R_G^\alpha(\tau, T) = \frac{G_\alpha(\tau, T)}{G_\alpha^{\mathrm{rec}}(\tau, T)}, \tag{21}$$

where the denominator is the so-called reconstructed correlator which is evaluated with the kernel $\mathcal{K}$ at temperature T, but with a 'reference' spectral function typically taken as the vacuum one (or at low temperature T^* where no significant medium modifications are expected).

3.3. Numerical results

Before turning to the numerical results for the finite-T spectral functions and correlator ratios let us briefly summarize our input quantities, largely as given in [10] (where more details can be found, including extensive analysis of the associated uncertainties). Our potentials (F or U) are based on fits to the lattice results for (2+1)-flavor QCD from [37]–[39] ('potential 1' in [10]). In vacuum our off-shell calculations reproduce the results of [10] since in the limit of vanishing c-quark width the propagator G_{12} reduces to the standard Thompson form. The bare charm-quark mass is set to $m_c^0 = 1.264\,\mathrm{GeV}$, which, together with a vacuum selfenergy of $X_\infty^{\mathrm{vac}}/2 = 0.6\,\mathrm{GeV}$, gives a fair description of the spin-average masses of J/ψ-η_c, ψ' and χ_c states.

The full off-shell treatment with more realistic c-quark propagators in the present work leads to moderate but significant changes for the in-medium results. In addition, the zero-mode contributions in the V, S and AV channels (recall equation (15)) have a marked impact on

the corresponding correlator ratios. For a comparison to lQCD correlator ratios we choose the results of the $N_f = 2$ computations from [36], which correspond more closely to our input potentials than quenched calculations. The critical temperature in the simulations of the lQCD correlator ratios [36] is $T_c \simeq 210\,\mathrm{MeV}$, which is not far from the one underlying our potential [37], $T_c \simeq 196\,\mathrm{MeV}$. Therefore, rather than normalizing to the different T_cs, we compare our results for the correlator ratios with the lQCD data in absolute units of Euclidean time, τ. Each correlator ratio is plotted up to the midpoint, $\tau = 1/2T$, of the total τ range (the correlators are symmetric about this point). Thus, comparable temperatures are easily identified by the same τ range in the plotted ratio (if one were to normalize all results to T_c, lQCD data at given absolute temperature would be compared to T-matrix calculations at slightly lower T).

The in-medium results using the internal energy, U, as potential are summarized in figure 1 in terms of the S- and P-wave spectral functions in the upper panels (degenerate for η_c-J/ψ and for χ_c states) and the correlator ratios in the middle and lower panels (where the degeneracies are lifted by the zero modes). Since the (magnitude of the) imaginary part of the selfconsistently calculated c-quark selfenergy turns out to be around 0.050–0.100 GeV for low-momentum on-shell charm quarks (cf figure 3 below), the closest comparison to our earlier quasiparticle results is for the case of a constant (energy and three-momentum independent) imaginary part of $\mathrm{Im}\,\Sigma_Q = -0.05\,\mathrm{GeV}$ (figure 14 in [10]). In the S-wave spectral function we find slightly more attraction for the ground-state peak for temperatures below $1.5\,T_c$ (for higher T it dissolves, as in [10]). Despite the larger on-shell width in our present treatment, which is up to twice as large as in our previous quasiparticle calculations, the width of the J/Ψ-η_c peaks is very similar. This is a direct consequence of the energy and momentum dependence of the selfenergy which decreases considerably off-shell (cf figure 3 below) and thus reduces the 'operative' width of c-quarks in $c\bar{c}$ bound states. It becomes apparent in the η_c correlator ratio (where no zero-mode is active), which at the lowest considered temperature ($1.2\,T_c$) drops to about 0.85 compared to 0.9 in [10], even though the peak position of the bound state is shifted to slightly lower energies in the present calculation (which tends to increase the large-τ correlator ratio). This finding shows that a proper off-shell treatment is warranted to correctly account for the low-energy strength in the spectral function, which has significant impact on the correlator ratio at large τ. We are not very concerned that the drop to 0.85 is noticeably larger than in the lQCD data since we have neglected several effects which will contribute further low-energy strength to the spectral function, e.g. imaginary parts in the c-quark selfenergy from scattering off thermal gluons, or coupled channels in the $c\bar{c}$ T-matrix such as $D\bar{D}$ and $c\bar{c}g$ (inducing singlet-to-octet transitions). These are expected to be especially relevant close to T_c (D-meson states will form close to T_c and gluo-dissociation is efficient for large charmonium binding, $E_B \geqslant T$). On the other hand, we note that the PS correlator ratio is remarkably independent of temperature and closer to one for intermediate and small τ than in [10] (e.g. no more than $\sim 2\%$ above one), which improves the agreement with lQCD. In the V, S and AV channels the zero-mode contributions lead to a marked enhancement of the correlator ratios at large τ, especially for the P-wave channels, where the c_1 coefficient is nonzero (for the vector channel, we sum over the spatial components only, corresponding to $\Gamma = \gamma_i$ in equation (15)). Compared to a zero-width treatment of the zero-mode contribution, corresponding to equation (19), the inclusion of a finite quark width increases the correlator ratios at large τ by about 0.1–0.15. Overall, the agreement of the calculated correlator ratios with $N_f = 2$ lQCD data [36] included in the middle and lower panels of figure 1 is fair. The largest discrepancies of about $\sim 30\%$ at both intermediate and large τ occur in the AV (χ_{c1}) channel, where the zero-mode contribution

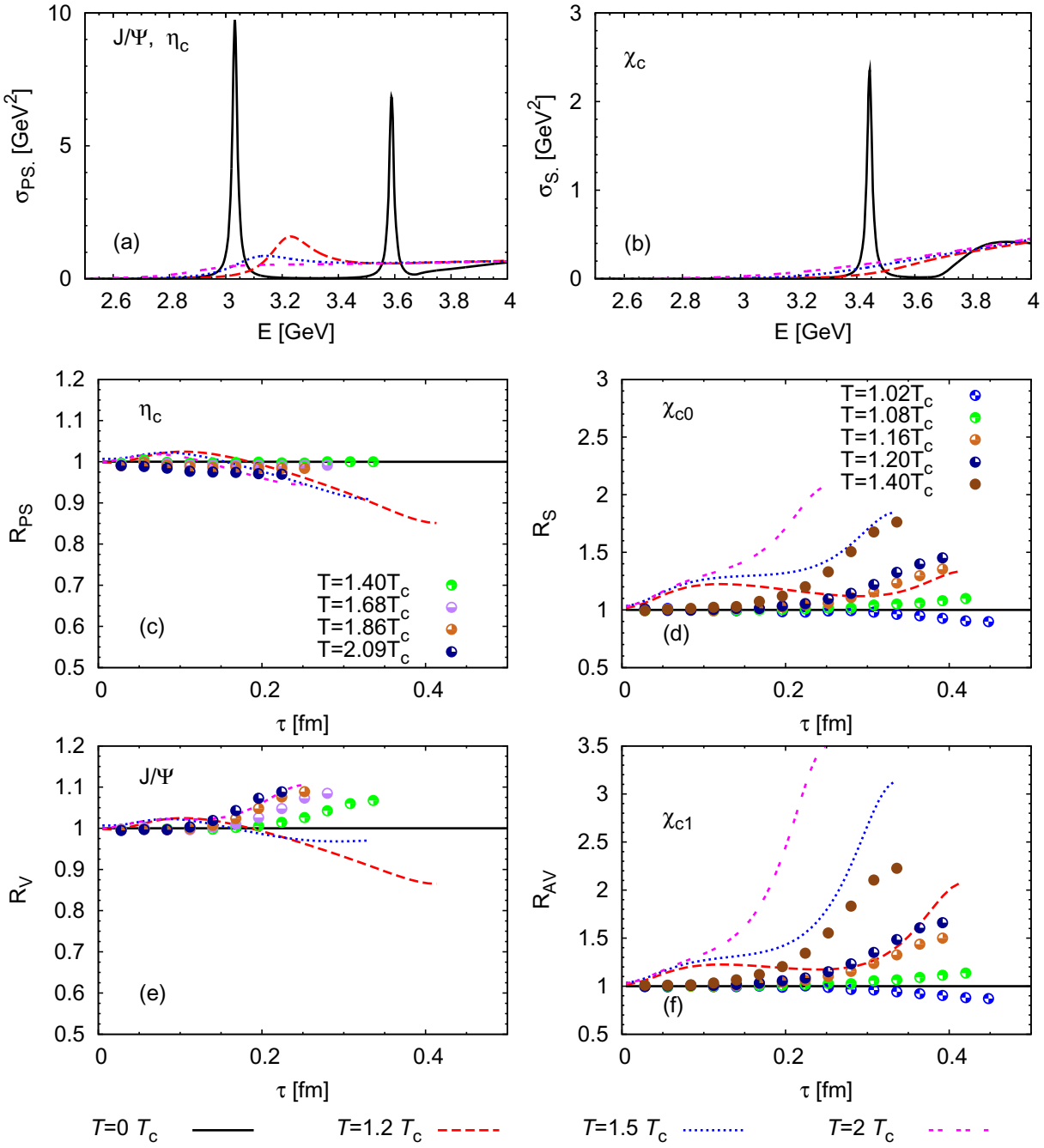

Figure 1. Charmonium spectral functions in the pseudoscalar (upper left panel) and scalar (upper right) channel for different temperatures using the internal energy, U, as $Q\bar{Q}$ potential. In the middle and lower rows we show the corresponding Euclidean correlator ratios in the pseudoscalar (middle left), scalar (middle right), vector (lower left) and axialvector channels (lower right), where the latter three include zero-mode contribution. The comparison to the lattice data (indicated by symbols) [36] is made in absolute units of τ (limited to $1/2T$ at each temperature), with $T_c \simeq 210\,\mathrm{MeV}$ for the lattice data and $T_c \simeq 196\,\mathrm{MeV}$ underlying the potential for the T-matrix calculations (e.g. 1.4 $T_c^{\mathrm{lat}} \simeq 1.5 T_c^{\mathrm{Tmat}}$).

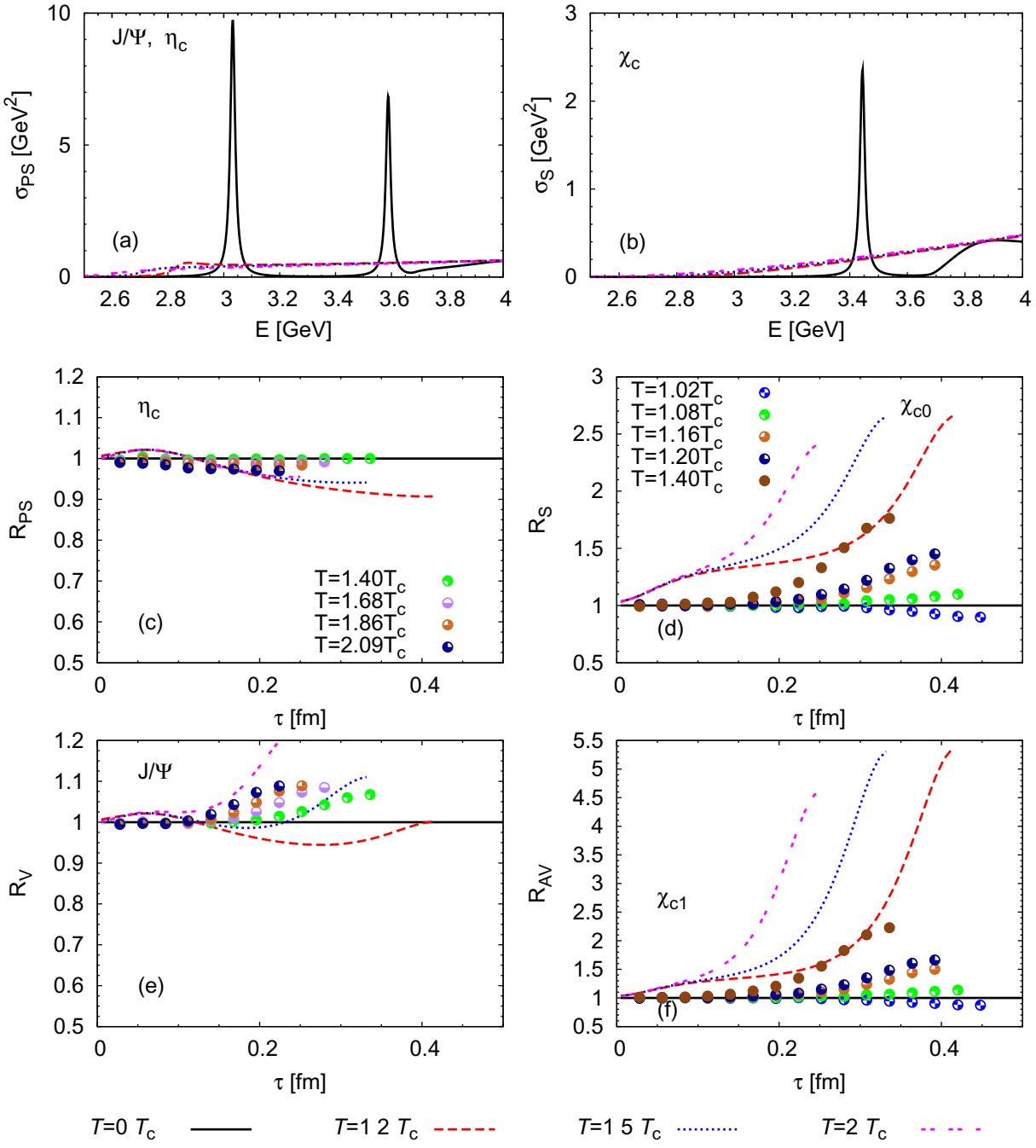

Figure 2. Same as figure 1 but using the free energy, F, as $Q\bar{Q}$ potential.

is the strongest. The extracted melting temperatures of the charmonium bound states are close to our earlier determination with finite but constant width [10], i.e. about 1.5 T_c for the J/Ψ and below 1.2 T_c for all other states (Ψ', χ_c).

The results obtained using the free energy, F, as potential are compiled in figure 2. As in previous work [9, 10, 40], we find a much stronger suppression of the bound states compared to using U, with a melting temperature for the S-wave ground state of 1.2 T_c or even lower, whereas the P-wave spectral function is already structureless at this temperature. Nevertheless,

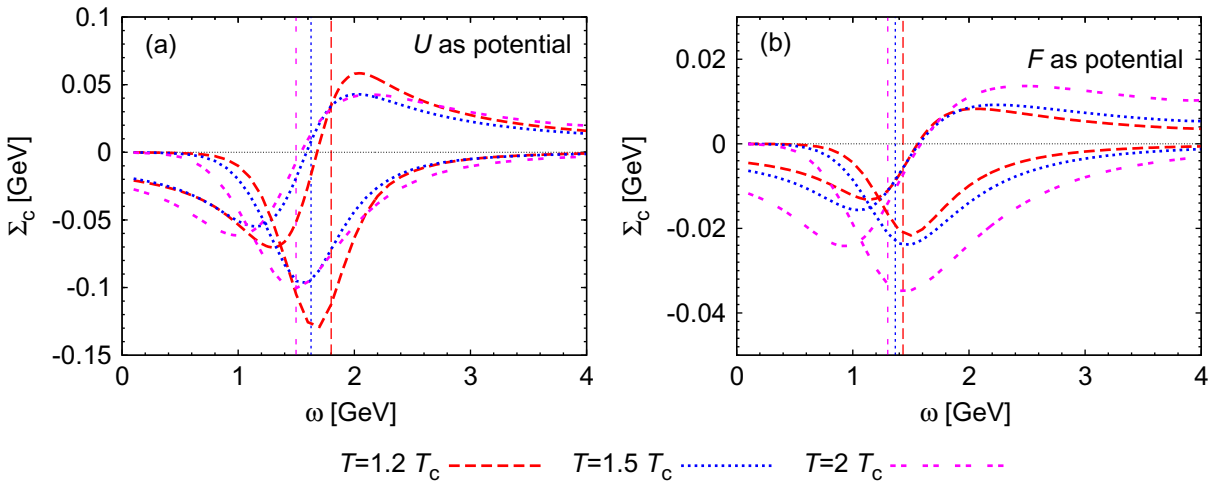

Figure 3. Real and imaginary parts of the charm-quark selfenergy at vanishing three-momentum in a QGP at different temperatures for the scenarios where the internal (left panel) or free energy (right panel) is employed as potential. The imaginary parts are negative definite, while the real parts change sign close to the vertical lines, which indicate the effective charm-quark mass (on-shell energy) at the respective temperature.

the correlator ratio in the η_c channel (no zero mode) is surprisingly T-stable and close to one: the loss of low-energy strength due to the dissolved bound state is compensated by a reduced $c\bar{c}$ threshold in connection with a nonperturbative rescattering strength in the threshold region generated through the T-matrix [8]. Indeed, the in-medium charm-quark mass (correction) following from equation (8) for F_∞ is significantly smaller than for U_∞. This, however, generates a markedly enhanced zero-mode contribution to the correlator ratios in the V, S and AV channels, compared to the case with U as potential (the effect of the selfconsistently calculated finite quark width in the zero modes is an about 10% enhancement at large τ). In particular, in the P-wave channels, the large-τ values exceed quite substantially the $N_f = 2$ lQCD data. Apparently a potential closer to the internal energy is favored (with larger m_c^* but stronger $c\bar{c}$ binding).

4. Open-charm transport

We now turn to examining the numerical results for the single charm-quark properties in the QGP, specifically its selfenergy (mass correction and scattering rate; section 4.1), thermal relaxation rate (section 4.2) and number susceptibility (section 4.3). We recall that these are selfconsistently computed via numerical iteration with the T-matrix in all heavy-light quark channels (equation (1)).

4.1. Selfenergy

The real and imaginary parts of the charm-quark selfenergy following from the T-matrix are displayed in figure 3 as a function of quark energy for vanishing three-momentum and for three temperatures. The general structure is that of a maximum around the on-shell energy,

$\omega \simeq m_c^*$, in the imaginary part, associated with a typical zero crossing in the real part. The peak structure is caused by Feshbach type resonances (or threshold enhancements) around the heavy-light quark threshold in the T-matrix [10, 14]. These features are the reason that, upon (off-shell) integration over ω in the two-particle propagator (T-matrix), the contributions from the real part largely cancel, while the width effects drop significantly more quickly (and thus on average are smaller) than for a constant quasiparticle particle width, as employed in previous work [8, 10, 14].

More quantitatively, in the case of U as potential (left panel in figure 3), the on-shell width of the charm quark reaches a value of up to $\Gamma_c = -2\,\mathrm{Im}\,\Sigma_c \simeq 250\,\mathrm{MeV}$ at the lowest considered temperature ($1.2\,T_c$), quite similar to what has been calculated in [14] using different lQCD inputs for U. The magnitude decreases with increasing temperature (not as much as in [14]), which is quite remarkable given the fact that the thermal densities of the thermal anti-/quarks decrease appreciably (in the 'T-ϱ' approximation, the selfenergy would be directly proportional to the light-quark density, $\Sigma_c \sim T_{cq} n_q$). It clearly reflects the weakening of the two-body interaction as temperature increases, due to color-charge screening in both the Coulomb and confining parts of the potential. In other words, the maximal interaction strength is realized at the lowest temperature, just above T_c.

For the F-potential the c-quark selfenergy is reduced by approximately a factor of 6 at the lowest temperature, which reduces to a factor of $\sim$2–3 at $2\,T_c$. In this scenario, no Feshbach resonances form, but rescattering embodied in the T-matrix still produces a notable threshold enhancement, which induces an on-shell width of about 40–70 MeV.

4.2. Thermal relaxation rate

Next we turn to the calculation of the thermal relaxation rate of charm quarks in the QGP, employing a Fokker–Planck treatment following [41]. The relation of the drag coefficient, $A(p)$, to the T-matrix has been elaborated in [14], including all color configurations in c-q and c-$\bar{q}$ scattering in S- and P-waves. For a more realistic evaluation of the total coefficient, we add to the T-matrix contribution the effect of c-quark scattering off thermal gluons, which we approximate with the leading order perturbative diagrams (using $\alpha_s = 0.4$), including Debye screening masses in the exchange propagators (t-channel gluon exchange gives the dominant contribution). In figure 4 the full results for $A(p)$ are compared to perturbative calculations in which scattering off both anti-/quarks and gluons is obtained from the LO diagrams. Compared to the quasiparticle treatment in [10], the full off-shell treatment leads to an approximately 10% increase of the drag coefficient at low three-momenta, while the deviations are small at momenta of $k \geqslant 2\,\mathrm{GeV}$. This is well in line with the finding in [10] that the dependence of the drag coefficient on the 3D reduction scheme of the T-matrix equation (relating to its off energy-shell behavior via different two-particle propagators) is small. Thus, we confirm as a robust feature that c-quark thermalization using the nonperturbative T-matrix is accelerated over pQCD calculations by about a factor of 4 (2) when using U (F) as potential.

In addition to the direct calculation of the relaxation rate following from the collision term in the Boltzmann (or Fokker–Planck) equation with the heavy-light T-matrix [10, 14], the off-shell framework set up in the present paper enables an alternative method, namely from the zero-energy limit of the heavy-quarkonium spectral function [11, 42],

$$\gamma_c = \frac{T}{m_c\, D_s}, \qquad D_s = \frac{1}{\chi_c(T)} \lim_{\omega \to 0} \frac{\rho_{\gamma_i}(\omega, 0)}{2\omega} \tag{22}$$

Table 1. Comparison of charm-quark relaxation rates, $\gamma_c(k=0;T)$, as obtained from the heavy-light T-matrix [10] (second column) and from a Kubo formula for the diffusion coefficient (third column) using the low-energy limit of the heavy-quarkonium spectral function, equation (22), for the two different scenarios for potential (upper and lower table). The last column lists a schematic estimate of the viscosity to entropy-density ratio using the kinetic-theory relation, equation (23), including the contributions from scattering off thermal gluons (the quoted ranges only reflect the variation in the two preceding columns; the true uncertainty is larger).

T (T_c)	Heavy-light T-matrix	Quarkonium spectral function	'η/s'
γ_c (1/fm) with U-potential			
1.2	0.137	0.177	0.16–0.2
1.5	0.136	0.148	0.28–0.3
2.0	0.180	0.147	0.41–0.47
γ_c (1/fm) with F-potential			
1.2	0.034	0.034	0.6
1.5	0.044	0.036	0.73–0.8
2.0	0.075	0.051	0.8–0.96

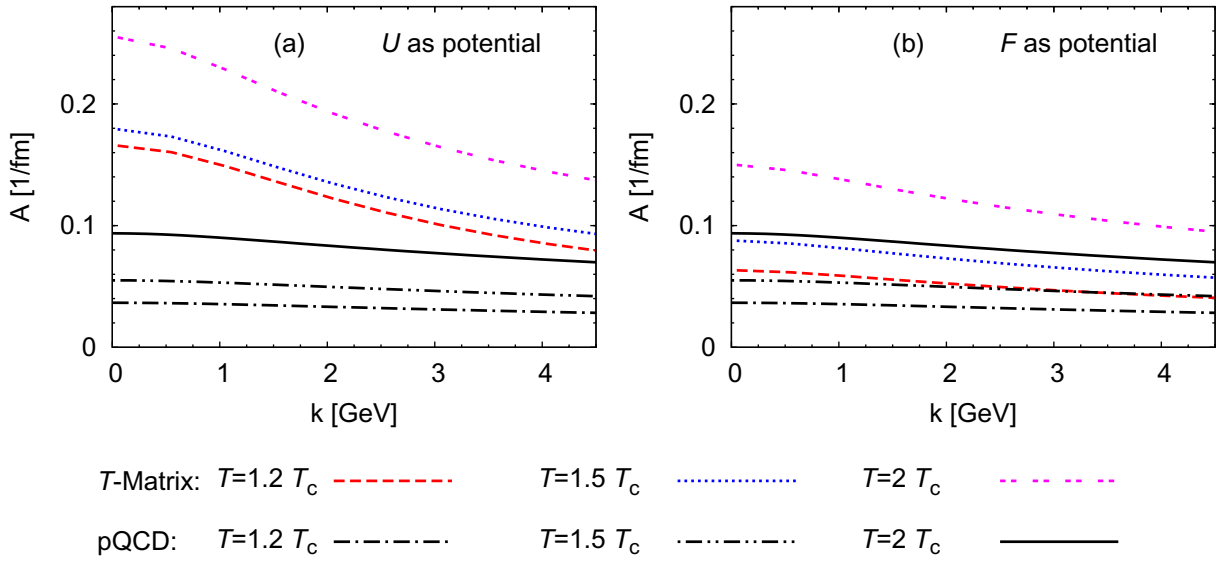

Figure 4. Charm-quark relaxation rate as a function of three-momentum for different temperatures using either the T-Matrix plus pQCD gluon scattering [10] (upper three lines in left panel) or a pQCD calculation for scattering off gluons and anti/quarks (lower three lines in left panel). The T-matrix is computed using U (left) or F (right) as potential while pQCD contributions are obtained with $\alpha_s = 0.4$.

($\chi_c \equiv \chi_{00}$: charm-quark number susceptibility, D_s: spatial diffusion constant). The values extracted from this method correspond to the zero-momentum limit and are compared to the pertinent values from the collision integral using the heavy-light T-matrix in table 1 (for a

consistent comparison the contribution from scattering off thermal gluons is not included). Note that the latter involves the Qq scattering amplitude squared, while the imaginary part of the quarkonium spectral function is basically determined by the imaginary part of the single-quark spectral function which, in turn, is obtained from the imaginary part of the heavy-light scattering amplitude, cf equation (10). We find that the extraction from the low-energy limit of the charmonium spectral function in the vector channel tends to give larger (smaller) values at lower (higher) for both U and F as two-body potential. One of the uncertainties which is presumably reflected by these deviations is the Fokker–Planck approximation when using the heavy-light T-matrix to evaluate the diffusion coefficient. For example, in [43] it has been found that a D-meson resonance model in the QGP can lead to a violation of the Einstein relation by underestimating γ_c by up to 10% at temperatures of $T \simeq 300\,\mathrm{MeV}$, while the agreement is closer at lower temperatures (less than 5% for $T < 250\,\mathrm{MeV}$; note that the D-meson like correlations in the T-matrix dissolve for temperatures above $1.5\,T_\mathrm{c} \simeq 300\,\mathrm{MeV}$). Overall, the discrepancies between the two methods are within $\sim 30\%$, which, given the different schemes of evaluating this transport coefficient, is not too bad. The systematic trends are similar when using F or U as potential, and the large difference between these two scenarios is robust.

Let us end this section by a schematic evaluation of the widely discussed ratio of viscosity to entropy density, η/s. Using kinetic theory, one can roughly relate this quantity to the spatial HQ diffusion coefficient as [3]

$$\frac{\eta}{s} \approx \frac{1}{5} T D_s. \tag{23}$$

The numerical coefficient probably constitutes a lower limit, applicable to a weakly coupled system; it is most likely larger for strongly coupled liquids, e.g. $\sim 1/2$ in gauge-gravity dual theories (AdS/CFT) [44]. Nevertheless, the results for U suggest that η/s is not far from the conjectured lower limit of 0.08 for quantum liquids. Moreover, its T-dependence seems to indicate a minimum value when approaching T_c from above, which would resemble rather generic behavior of substances in the vicinity of a critical point. This feature is also present for the F-potential, albeit the T-dependence is less pronounced; of course, the values are also much larger compared to the U-potential, by approximately a factor of 2–4. In fact, the η/s value for F at $2\,T_\mathrm{c}$ is quite close to perturbative calculations [45, 46] where $\eta/s \simeq 1$ with little T-dependence, indicating that resummation effects in the T-matrix do not play a large role under these conditions.

4.3. Charm-quark number susceptibility

Quark-number susceptibilities, χ_q, which we already utilized in connection with the c-quark diffusion coefficient, equation (22), can be computed quite accurately in lQCD [47] and are therefore of great interest to constrain effective models of the QGP. For example, HQ number susceptibilities have been used to extract effective in-medium charm- and bottom-quark mass corrections by fitting a zero-width quasiparticle expression, equation (19), to the lQCD results [48]. Here, we carry out a full off-shell calculation including finite-width effects through the single c-quark propagators figuring into the charmonium spectral function [49],

$$\chi_c(T) = \frac{1}{T} \int_0^\infty \frac{\mathrm{d}E}{2\pi} \frac{2}{1 - \exp(-E/T)} \rho_{00}(E, \mathbf{0}). \tag{24}$$

For high $T \gg m_Q$, Σ_Q, this quantity reduces to

$$\chi_c(T) = \frac{2\,N_c}{6}\,T^2. \tag{25}$$

In figure 5 we summarize our results for the HQ susceptibility and compare to lQCD data as well as the zero-width quasiparticle limit (equation (19)) used in previous estimates. When plotted as a function of temperature over in-medium c-quark mass (left panel), the results for the U-potential are slightly above those for F (note that the in-medium c-quark mass is 10–20% larger for the U-potential, mostly due to the larger mass correction resulting from $U_\infty/2$ compared to $F_\infty/2$). The full results using U are significantly above an off-shell calculation where the imaginary parts are put to zero, which in turn agree very well with the zero-width quasiparticle limit (dashed line). When plotted as a function of temperature (right panel in figure 5), it turns out that the results for F are somewhat above those for U, due to the smaller $m_c(T)$. On the other hand, the finite-width effects in the full results using U produce an increase in χ_c over the no-width limit, which corresponds to a c-quark mass decrease of approximately 150–200 MeV in the zero-width quasiparticle expression. Thus, finite widths considerably affect the extraction of the in-medium c-quark mass from the susceptibility. This effect also leads to a significant improvement in the comparison to lQCD results: the full results with U roughly lie in the uncertainty band encompassed by the lQCD results, while the full results with F tend to lie at the upper end of that band. At the lowest considered temperature, the results for U seem to lie below the $N_t = 8$ lQCD computations, but as indicated in connection with the large-τ limit of the S-wave charmonium correlator ratios, we believe that further width (and coupled-channel) corrections need to be included close to T_c before more precise conclusions can be drawn. At least the underestimate of the lQCD data in our calculations for χ_c and the large-τ limit of $R_{PS,V}$ is consistent.

5. Conclusions

We have conducted a study of charmonium and open-charm properties in the QGP using a thermodynamic T-Matrix formalism. For the first time in the context of heavy quarks in the QGP, we have implemented this scheme selfconsistently at the one- and two-body level (i.e. selfenergy and scattering amplitude), including microscopically calculated off-shell effects, in particular imaginary parts. Within the Matsubara formalism, the two-particle propagator in the T-matrix equation automatically generates 'zero-mode' contributions, i.e. scattering off pre-existing charm quarks in the heat bath. Following our earlier work [10], the two-body input potential was constructed using a field-theoretical model for Coulomb and confining forces with its four parameters fitted to finite-temperature lQCD data of the color-averaged HQ free energy. As limiting cases of the interaction strength we have considered the resulting free and internal energy as an underlying potential. Once the input potential and the bare charm-quark mass are fixed (the latter is adjusted to reproduce the charmonium ground-state mass in vacuum), there are no further tunable parameters in the heavy-heavy and heavy-light sector of our approach; HQ interactions with gluons are treated perturbatively but turn out to play a minor role (even with $\alpha_s = 0.4$). We are then able to comprehensively compute hadronic spectral functions in different charmonium and D-meson channels, as well as HQ selfenergies and transport properties in the QGP. Specifically, we have applied these quantities to calculate Euclidean correlator ratios for charmonia (consistently including zero-modes in scalar and axial/vector channels) and the

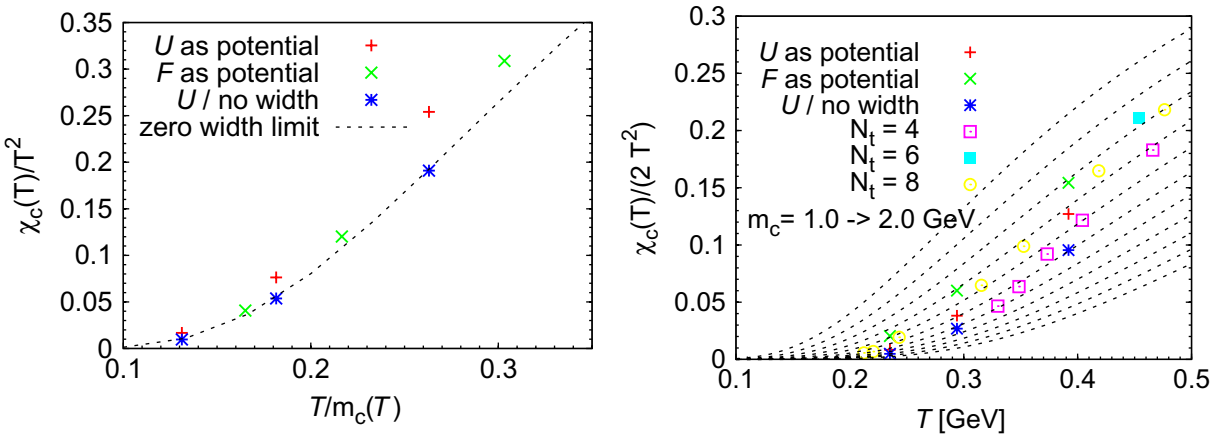

Figure 5. Charm-quark number susceptibility as a function of temperature normalized to the zero mass limit, equation (25). Left panel: comparison of our full off-shell calculations with finite width (using either U or F as potential) to the zero width-limit using U and the quasiparticle expression, equation (19), with T-dependent c-quark mass; the temperature on the x-axis has been rescaled by the respective in-medium masses in each scenario. Right panel: comparison of our results to lattice computations in 2+1-flavor QCD with different numbers, N_t, of lattice points in temporal direction; the dashed lines indicate the zero-width quasiparticle results using equation (19) for fixed c-quark mass, increasing in steps of 0.1 GeV from top to bottom.

charm-quark number susceptibility, which have both been 'measured' with good accuracy in thermal lQCD. Overall, we find an encouraging degree of agreement between our results and those in lQCD, especially at temperatures $T \geqslant 1.5\,T_c$ (possibly with a preference for using U as potential), keeping in mind that neither F nor U, as computed in lQCD, necessarily provide a rigorous definition of a two-body potential, as both quantities are computed from differences of thermal averages. Especially close to T_c a more complete description of charm and charmonia remains a challenge, requiring further refinements such as the inclusion of (pre-) hadronic states in the QQ and Qq T-matrices (coupled channels), a nonperturbative treatment of interactions with thermal gluons and a careful assessment of retardation effects. The large entropy contribution in the HQ free energy close to T_c indeed suggests many additional states to play a role. Another extension of our approach concerns the three-momentum dependence of charmonium correlators/spectral functions, for which interesting lQCD results are now becoming available [50].

Our analyses and findings reveal the intricate relation between charmonium bound-state properties and HQ diffusion in the QGP, which, in particular, cannot be captured by perturbative treatments. The very same (resummed) force that generates resonance-like correlations (or threshold enhancements) in charmonium spectral functions—crucial for properly describing the lQCD correlator ratios—is operative in low-momentum charm-quark scattering (closely related to zero modes), and thus most likely instrumental in reducing the pertinent thermal relaxation times, as required in phenomenological applications to RHIC data [14, 51]. It remains an open question how large c-quark momenta need to be for radiative processes to become competitive with elastic scattering [1, 52].

In conclusion, we believe that studying the many-body physics of HQ systems in the QGP can indeed reveal valuable insights into the medium modifications of the basic QCD force via its effects on bound-state properties and heavy-flavor transport. The nonperturbative nature of the problem, especially in the vicinity of T_c, requires effective approaches whose predictive power greatly benefits from constraints obtained from thermal lQCD. This will hopefully pave the way toward illuminating and quantifying the properties of the QGP even in the case of rather strong coupling, and help understand some of the fascinating phenomena observed in ultrarelativistic heavy-ion collisions.

Acknowledgments

The authors acknowledge useful discussions with M He and X Zhao, and are indebted to J I Skullerud for providing the lattice-QCD data on the charmonium correlator ratios. This work has been supported by the US National Science Foundation under CAREER grant No. PHY-0449489 and grant no. PHY-0969394, and by the A-v-Humboldt Foundation.

References

[1] Rapp R and van Hees H 2010 *Quark-Gluon Plasma* 4th ed R Hwa and X N Wang (Singapore: World Scientific) 111 (arXiv:0903.1096 [hep-ph])
[2] Satz H 2006 *J. Phys. G: Nucl. Part. Phys.* **32** R25
[3] Rapp R, Blaschke D and Crochet P 2010 *Prog. Part. Nucl. Phys.* **65** 209
[4] Bazavov A, Petreczky P and Velytsky A 2010 *Quark-Gluon Plasma* 4th ed R Hwa and X N Wang (Singapore: World Scientific) p 61 (arXiv:0904.1748 [hep-ph])
[5] Braun-Munzinger P and Stachel J 2009 *Relativistic Heavy-Ion Physics* ed R Stock and Landolt-Börnstein (Berlin: Springer) (New Series 1–23A) arXiv:0901.2500 [nucl-th]
[6] Kluberg L and Satz H 2009 *Relativistic Heavy-Ion Physics* ed R Stock and Landolt-Börnstein (Berlin: Springer) (New Series 1–23A) (arXiv:0901.4014 [hep-ph])
[7] Wong C Y and Crater H W 2007 *Phys. Rev.* D **75** 034505
[8] Cabrera D and Rapp R 2007 *Phys. Rev.* D **76** 114506
[9] Mocsy A and Petreczky P 2007 *Phys. Rev. Lett.* **99** 211602
Mocsy A and Petreczky P 2008 *Phys. Rev.* D **77** 014501
[10] Riek F and Rapp R 2010 *Phys. Rev.* C **82** 035201
[11] Petreczky P and Teaney D 2006 *Phys. Rev.* D **73** 014508
[12] Aarts G and Martinez Resco J M 2005 *Nucl. Phys.* B **726** 93
[13] Umeda T 2007 *Phys. Rev.* D **75** 094502
[14] van Hees H, Mannarelli M, Greco V and Rapp R 2008 *Phys. Rev. Lett.* **100** 192301
[15] Alberico W M, Beraudo A, De Pace A and Molinari A 2008 *Phys. Rev.* D **77** 017502
[16] Rapp R, Cabrera D, Greco V, Mannarelli M and van Hees H 2008 *Proc. 24th Winter Workshop on Nuclear Dynamics* (*South Padre Island, TX, 5–12 April, 2008*) arXiv:0806.3341 [hep-ph]
[17] Mannarelli M and Rapp R 2005 *Phys. Rev.* C **72** 064905
[18] Yaes R J 1971 *Phys. Rev.* D **3** 3086
[19] Frohlich J, Schwarz K and Zingl H F K 1983 *Phys. Rev.* C **27** 265
[20] Blankenbecler R and Sugar R 1966 *Phys. Rev.* **142** 1051
[21] Thompson R H 1970 *Phys. Rev.* D **1** 110
[22] Megias E, Ruiz-Arriola E and Salcedo L L 2007 *Phys. Rev.* D **75** 105019
[23] Brown G E, Lee C-H, Rho M and Shuryak E 2004 *Nucl. Phys.* A **740** 171
[24] Shuryak E V and Zahed I 2004 *Phys. Rev.* D **70** 054507

[25] Brown G E 1952 *Philos. Mag.* **43** 467
[26] Beraudo A, Blaizot J P, Garberoglio G and Faccioli P 2009 *Nucl. Phys.* A **830** 319c
[27] Cassing W 2007 *Nucl. Phys.* A **795** 70–97
[28] Rapp R and Wambach J 1995 *Phys. Lett.* B **351** 50
[29] Beraudo A, Blaizot J P and Ratti C 2008 *Nucl. Phys.* A **806** 312
[30] Brambilla N, Ghiglieri J, Vairo A and Petreczky P 2008 *Phys. Rev.* D **78** 014017
[31] Laine M, Philipsen O, Romatschke P and Tassler M 2007 *J. High Energy Phys.* JHEP03(2007)054
[32] Rothkopf A, Hatsuda T and Sasaki S 2009 *PoS* **LAT2009** 162
[33] Bhanot G and Peskin M E 1979 *Nucl. Phys.* B **156** 391
[34] Grandchamp L and Rapp R 2001 *Phys. Lett.* B **523** 60
[35] Jakovac A, Petreczky P, Petrov K and Velytsky A 2007 *Phys. Rev.* D **75** 014506
[36] Aarts G, Allton C, Oktay M B, Peardon M and Skullerud J-I 2007 *Phys. Rev.* D **76** 094513
[37] Kaczmarek O 2007 *PoS* **CPOD07** 043
[38] Cheng M *et al* 2008 *Phys. Rev.* D **77** 014511
[39] Kaczmarek O 2009 private comunication
[40] Mocsy A and Petreczky P 2006 *Phys. Rev.* D **73** 074007
[41] Svetitsky B 1988 *Phys. Rev.* D **37** 2484
[42] Caron-Huot S, Laine M and Moore G D 2009 *J. High Energy Phys.* JHEP04(2009)053
[43] van Hees H and Rapp R 2005 *Phys. Rev.* C **71** 034907
[44] Herzog C P, Karch A, Kovtun P, Kozcaz C and Yaffe L G 2006 *J. High Energy Phys.* JHEP07(2006)013
[45] Blaizot J P and Iancu E 1999 *Nucl. Phys.* B **557** 183
[46] Arnold P, Moore G D and Yaffe L G 2003 *J. High Energy Phys.* JHEP05(2003)051
[47] Petreczky P, Hegde P and A Velytsky 2009 *PoS* **LAT2009** 159 (RBC-Bielefeld Collaboration)
[48] Petreczky P 2009 *Eur. Phys. J.* C **62** 85
[49] Hatsuda T and Kunihiro T 1994 *Phys. Rep.* **247** 221
[50] Asakawa M *Talk at INT Program 10-2a on 'Quantifying the properties of QCD Matter' (Seattle, WA, 24 May to 16 July 2010)*
Oktay M B and Skullerud J-I 2010 arXiv:1005.1209 [hep-ph]
[51] van Hees H, Greco V and Rapp R 2006 *Phys. Rev.* C **73** 034913
[52] Vitev I, Adil A and van Hees H 2007 *J. Phys. G: Nucl. Part. Phys.* **34** S769